JOURNAL OF SOLID STATE CHEMISTRY 21, 135–143 (1977)

$LaRu_xFe_{1-x}O_3$ Perovskites

R. J. BOUCHARD, J. F. WEIHER, AND J. L. GILLSON

E. I. du Pont Nemours and Company, Central Research and Development Department, Experimental Station, Wilmington, Delaware 19898

Received December 10, 1976; in final form January 27, 1977

To complete a study of $LaRuO_3$-based phases, a series of $LaRu_xFe_{1-x}O_3$ solid solutions was prepared with the orthorhombic $GdFeO_3$-type perovskite structure. Electrical, magnetic, crystallographic, and Mössbauer data were taken. Metallic conductivity is destroyed by substitution of as little as 10% Fe for Ru. Mössbauer and magnetic data show the presence of only high-spin octahedral Fe^{3+}. At the Fe-rich end, Ru decreases T_N of $LaFeO_3$ by $\approx 100°C$ for every 10% of Ru.

Introduction

We have previously investigated two perovskite solid solutions based on antiferromagnetic,[1] metallic $LaRuO_3$; $La_xSr_{1-x}RuO_3$ (*1*) with $SrRuO_3$, a ferromagnetic metal, and $LaRu_xGa_{1-x}O_3$ (*2*) with $LaGaO_3$, a diamagnetic insulator. In the former case, the ferromagnetism of $SrRuO_3$ was destroyed at ~35 mole% La, but metallic conductivity was maintained for all La/Sr ratios. In the latter, semiconduction occurred when only 10% of the Ru was substituted by Ga, and a temperature-dependent magnetic moment was found for the Ru^{3+}. The third solid-solution series, $LaRu_xFe_{1-x}O_3$, was designed to answer the following questions: (1) Will the high conductivity of $LaRuO_3$ be destroyed by the introduction of a small amount of Fe^{3+} on the *B* site as in the Ga^{3+} case, or will the Fe^{3+}, which has unpaired *d* electrons, maintain conductivity over a more extended range? (2) Will the conductivity vs temperature behavior be a monotonic function of x or would discontinuous properties be observed? (3) Will a metal–semiconductor transition be observed at some critical Ru^{3+} concentration? (4) Will localized Fe^{3+} electrons enhance the weak antiferromagnetic Ru^{3+}–Ru^{3+} interaction? (5) How fast will Ru^{3+} decrease the strong Fe^{3+}–Fe^{3+} antiferromagnetic exchange?

We felt that a crystal-chemical, magnetic, electrical, and Mössbauer investigation would provide answers to these questions.

Experimental

Mixtures of reagent-grade oxides were ground for ~30 min in a Fisher automatic agate mortar and pestle under N_2 according to the following equation:

$$2\,La_2O_3 + 2(1-x)Fe_2O_3 + 3xRuO_2 + xRu \rightarrow 4\,LaRu_xFe_{1-x}O_3.$$

The La_2O_3 was predried at 900°C, stored in a vacuum desiccator before use, then weighed as quickly as possible. The ground oxide mixtures were pelleted in a hand press, heated to ~600°C in a silica tube under a vacuum (to remove any small amounts of H_2O and CO_2 picked up during grinding and pressing), then sealed in Pt tubes under vacuum and fired to 1350°C for ~2 days. The pellets were fairly well sintered and colored black (high Ru content) to brown (high Fe content). Standard four-probe resistivity measurements were made on the pellets

[1] The description of $LaRuO_3$ as weakly antiferromagnetic may be open to question–a theta of −30K seems to resolve some complex magnetic behavior (*2*). However, Greenwood *et al.* (Abstracts of International Mössbauer Conference, Corfu, 1976) see no magnetic order in the ^{99}Ru Mössbauer spectrum at 4.2K.

ISSN 0022-4596

TABLE 1

LATTICE PARAMETERS VS COMPOSITION

Formula	a (Å)	b (Å)	c (Å)	v (Å^3)
$LaFeO_3$	5.5551(6)	5.5650(5)	7.8524(16)	242.75(4)
$LaRu_{0.05}Fe_{0.95}O_3$	5.5608(12)	5.5653(18)	7.8591(9)	243.22(8)
$LaRu_{0.1}Fe_{0.9}O_3$	5.5622(5)	5.5667(5)	7.8642(12)	243.50(4)
$LaRu_{0.15}Fe_{0.85}O_3$	5.5633(13)	5.5741(8)	7.8636(16)	243.85(6)
$LaRu_{0.2}Fe_{0.8}O_3$	5.5605(10)	5.5808(5)	7.8658(15)	244.09(5)
$LaRu_{0.25}Fe_{0.75}O_3$	5.5667(10)	5.5804(11)	7.8704(11)	244.49(5)
$LaRu_{0.4}Fe_{0.6}O_3$	5.5698(13)	5.5944(5)	7.8786(14)	245.49(5)
$LaRu_{0.5}Fe_{0.5}O_3$	5.5676(8)	5.6054(8)	7.8829(12)	246.01(4)
$LaRu_{0.6}Fe_{0.4}O_3$	5.5601(6)	5.6376(6)	7.8790(9)	246.97(3)
$LaRu_{0.8}Fe_{0.2}O_3$	5.5386(4)	5.6928(4)	7.8685(7)	248.09(2)
$LaRuO_3$	5.4944(6)	5.7789(5)	7.8548(7)	249.40(3)

and a Faraday balance was used to obtain magnetic data.

A Guinier–Hägg camera with KCl as an internal standard was used to determine accurate d values, which were refined by a least-quares procedure for accurate lattice parameters.

Mössbauer spectra were obtained with a NSEC-AM1 constant acceleration drive, a Reuter–Stokes Kr–CO_2 filled proportional counter, a Nuclear Data ND-180 Multichannel Analyzer in the time mode, and 15 mCi of ^{57}Co in a Cu-foil source. The velocity and isomer shift scales were calibrated with a NBS metallic Fe Mössbauer standard. The isomer shift of the source relative to Fe metal was 0.218 ± 0.002 mm/sec. Spectra were fit with a least-squares computer program assuming Lorentzian line shapes.

Results

Crystallographic

A complete range of single-phase $LaRu_xFe_{1-x}O_3$ solid solutions could be prepared. All compounds have the orthorhombic $GdFeO_3$-type structure, D_{2h}^{16}-*Pbnm*, $Z = 4$, as did the previous two solid solution series based on $LaRuO_3$. Our cell parameters for $LaFeO_3$ compare well with those in the literature (*4*). Lattice parameters vs x are

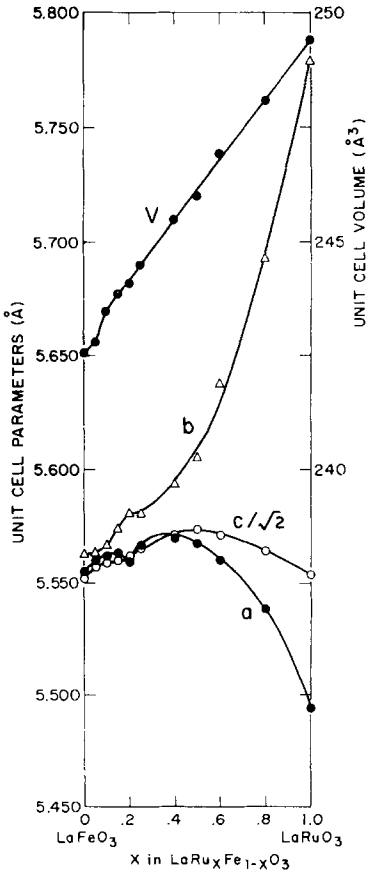

FIG. 1. Lattice parameters vs composition.

listed in Table I and illustrated in Fig. 1. They do not behave exactly like those in the previous solid solutions studied, e.g., there is no region where $b < a$, and the parameters do not vary smoothly—there are "kinks" in the curves. Otherwise, the gross features are similar to those of $LaRu_xGa_{1-x}O_3$ (*2*) and $La_xSr_{1-x}RuO_3$ (*1*), e.g., the b axis decreases rapidly with substitution into $LaRuO_3$. The anomalous behavior of $LaRu_xFe_{1-x}O_3$ is probably caused by a magnetostrictive contribution to the lattice constant, since in this composition range where the anomalies occur, the Néel temperatures rise above room temperature, where the lattice parameters are determined.

Electrical

Figure 2 shows resistivity vs temperature for the solid solutions. All are semiconducting except for the end member $LaRuO_3$. There is a fairly monotonic change from semiconducting $LaFeO_3$ to metallic $LaRuO_3$. Figures 3 and 4 and Table II show the smooth variation in room temperature resistivity and activation energy with x. Most of the plots of ρ vs T show more than one activation energy (Fig. 2)—the higher temperature activation energies are the ones plotted in Fig. 4. Breaks in ρ vs T plots for $LnFeO_3$-type perovskites at T_N are known in the literature (*5*). $LaFeO_3$ was not measured, but is known (*5*) to have $E_a = 0.22$ eV.

The electrical properties observed are similar to those for $LaRu_xGa_{1-x}O_3$ (*2*). No discontinuous behavior or metal–semiconductor transition is exhibited. In addition, as with Ga^{3+}, a small amount of Fe^{3+} is sufficient to cause semiconductivity. If anything, Fe substitution destroys the metallic conductivity of $LaRuO_3$ at lower concentrations than Ga^{3+}. This is surprising, since Fe^{3+} has 5 *d*-electrons like Ru^{3+} and $LaFeO_3$

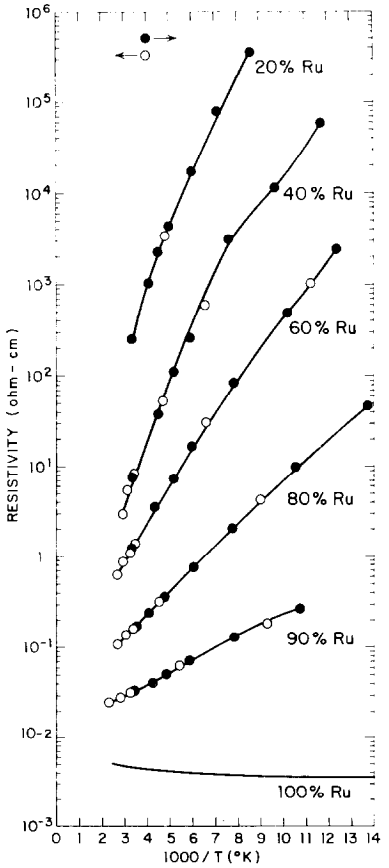

FIG. 2. Resistivity vs temperature as a function of composition.

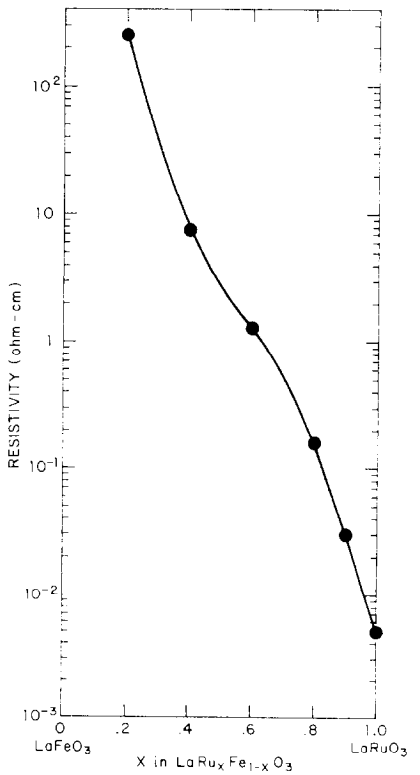

FIG. 3. Resistivity at 25°C vs composition.

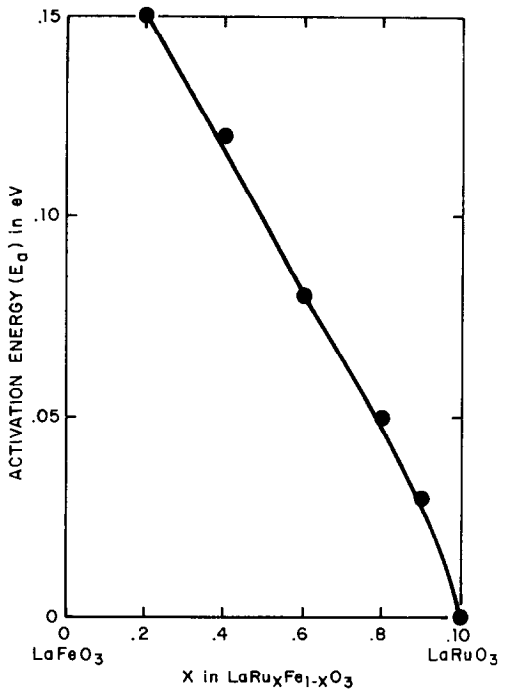

FIG. 4. Activation energy vs composition.

TABLE II

ELECTRICAL DATA

Formula	Resistivity at 25°C (ohm-cm)	Activation energy (eV)
$LaRuO_3$	5×10^{-3}	~0
$LaRu_{0.9}Fe_{0.1}O_3$	3×10^{-2}	0.03
$LaRu_{0.8}Fe_{0.2}O_3$	1.6×10^{-1}	0.05
$LaRu_{0.6}Fe_{0.4}O_3$	1.3	0.08
$LaRu_{0.4}Fe_{0.6}O_3$	7.6	0.12
$LaRu_{0.2}Fe_{0.8}O_3$	250	0.15

is much more conductive than $LaGaO_3$, which is essentially an insulator. Since the data used in the plots were those taken above T_N, no magnetic ordering contribution to localization is likely to be important.

The data represent a good illustration of the marked increase in metal–oxygen covalence of 4*d* vs 3*d* orbitals. The metallic conductivity in all $ARuO_3$-type perovskites presumably arises from the partially filled Ru–O π^* band. When the Ru sublattice is interrupted by even a small amount (<10%) of Fe, the metallic conductivity is destroyed, in spite of the fact that Fe^{3+} has 5 *d*-electrons like Ru^{3+} (d^5) and the unit cell volume decreases with Fe substitution.

It is interesting to compare these data with those recently published on $SrFe_xRu_{1-x}O_{3-y}$ (*6*). The latter solid solutions are complicated by the presence of oxygen vacancies and the fact that measurements were done on compacted powders, not sintered samples. Nevertheless, low resistivities appear to be maintained at higher Fe concentrations than for $LaFe_xRu_{1-x}O_3$. This probably reflects the stronger covalency resulting when higher Ru valence states are present. This also seems to be true for the 50% Ru^{4+} case in $LaRu_{0.5}Ni_{0.5}O_3$ and $LaRu_{0.5}Mg_{0.5}O_3$, where low resistivities are observed (*3*).

TABLE III

MAGNETIC DATA

Formula	μ_{Fe}[a]	ΔT[b]
$LaFe_{0.2}Ru_{0.8}O_3$	5.8 ± 0.1	300–100
$LaFe_{0.4}Ru_{0.6}O_3$	5.1 ± 0.1	300–200

[a] $\mu_2 = \mu^2_{Fe}(\bar{x}_{Fe}) + \mu^2_{Ru}(\bar{x}_{Ru})$ where $\bar{x}$ = mole fraction.
[b] Temperature interval used in μ calculation.

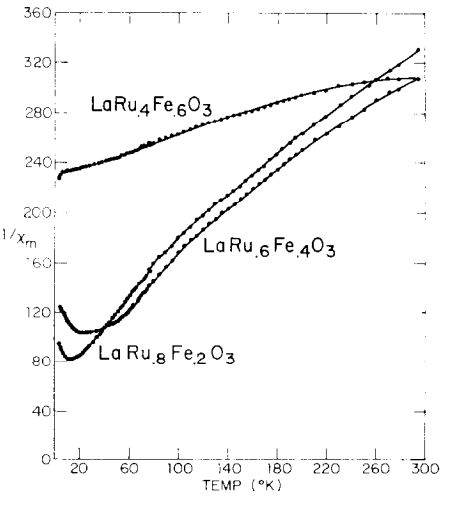

FIG. 5. Magnetic susceptibility of the mostly paramagnetic solid solutions.

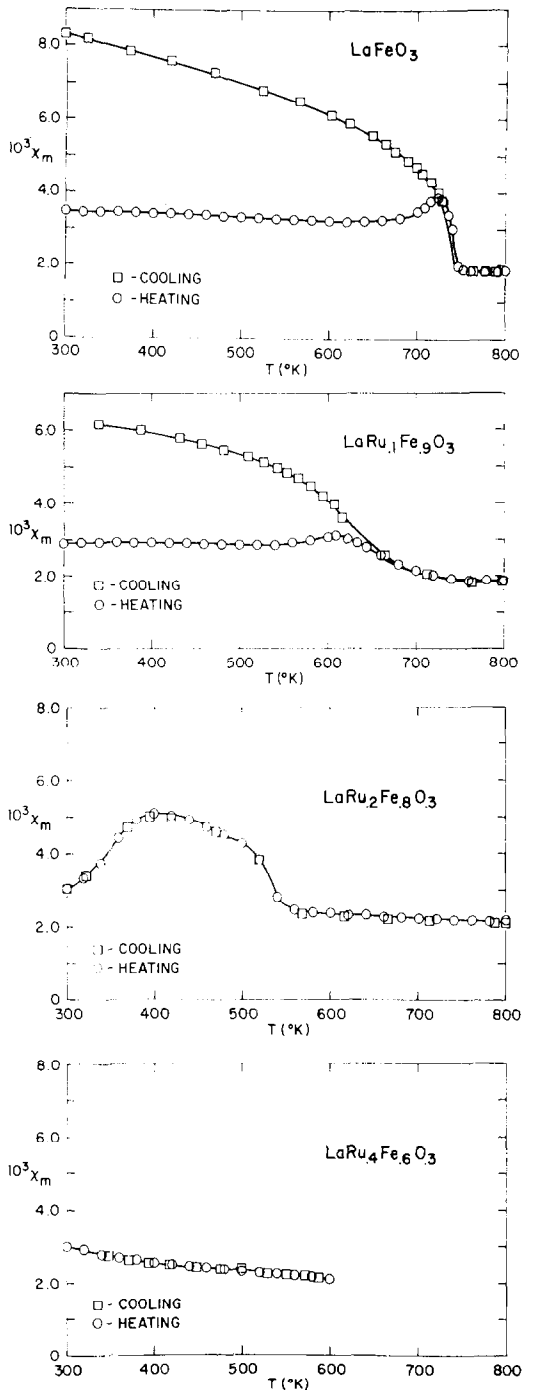

FIG. 6. Magnetic susceptibility of the mostly antiferromagnetic solid solutions.

Magnetic

Because of the antiferromagnetic nature of these solid solutions, only those with low Fe content (and consequently low T_N) were studied for paramagnetism below room temperature. Data are shown in Table III and Fig. 5. The Fe^{3+} moments are derived assuming a Ru moment of 2.12, the average Ru moment found in the $LaRu_xGa_{1-x}O_3$ series (*2*). The moment in the 20% Fe compound is close to the 5.92 BM expected for high-spin octahedral Fe^{3+}. A lower moment is found in the 40% Fe compound, but this may not be a real effect, since the straight line portion of the $1/\chi$ vs T curve is so short. In any case, the introduction of up to 40 mole% Fe does not change the magnetic properties of $LaRuO_3$ very dramatically—only a small increase in T_N is noted. At 60% Fe, T_N increases considerably, and although ill-defined, appears to be ≈ 300 K.

At the Fe-rich end of the series, measurements were done at higher temperatures and shown in Fig. 6. For these compounds it is more relevant to plot susceptibility, which is proportional to magnetization ($\chi = M/H$), rather than the $1/\chi$ vs T plots appropriate for paramagnets. For $LaFeO_3$ and $LaRu_{0.1}Fe_{0.9}O_3$ there are two curves, one obtained on

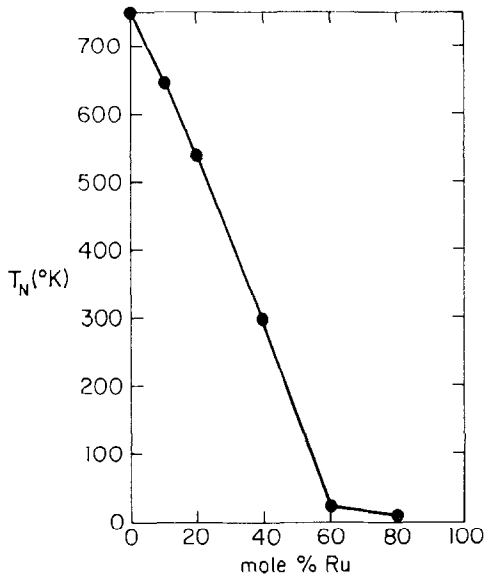

FIG. 7. Néel temperature vs Ru content.

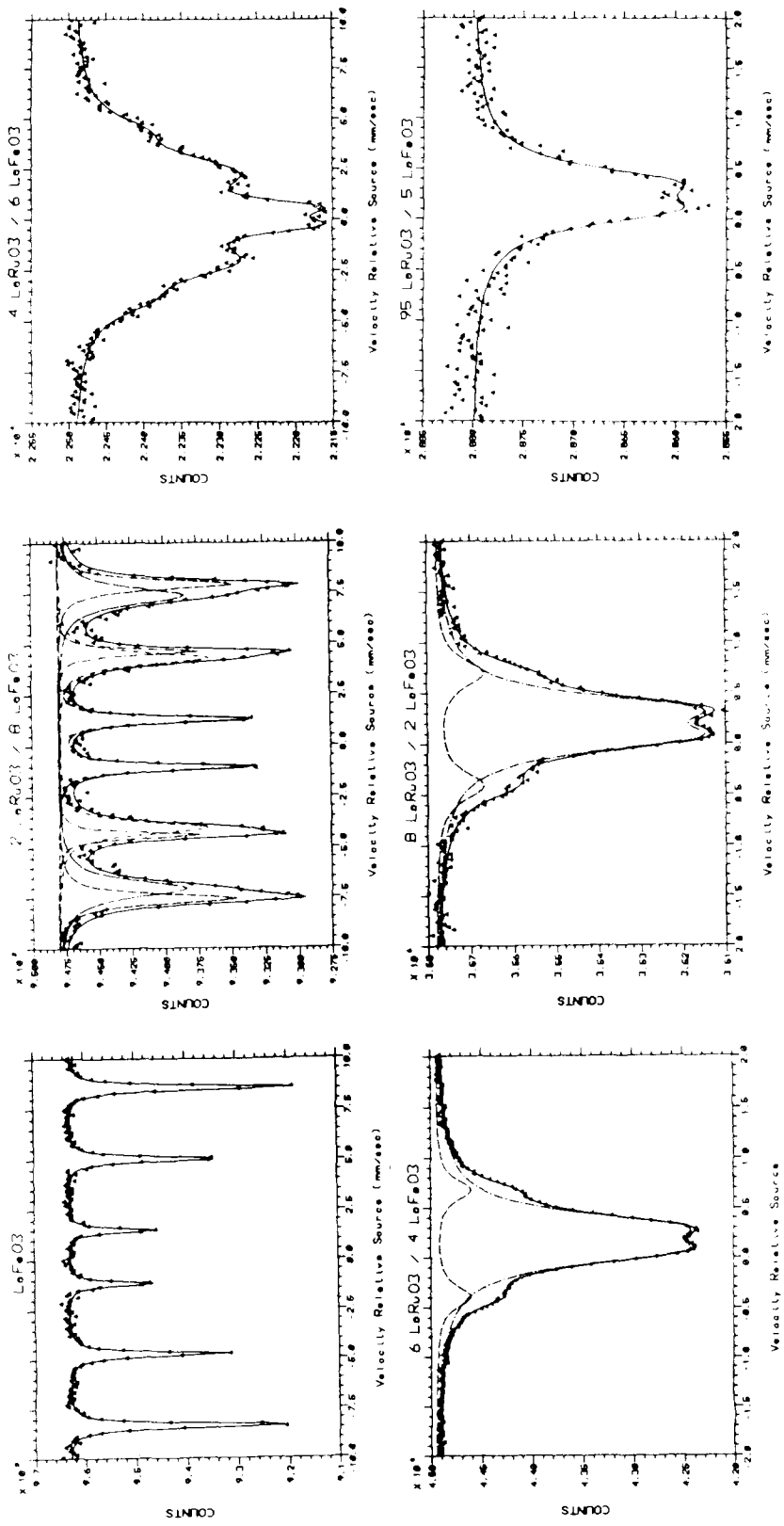

FIG. 8. Mössbauer spectra vs composition.

TABLE IV

MÖSSBAUER DATA

Mole % Fe	Type 1			Type 2				
	I.S.[a]	ΔE_Q[b]	Hi[c]	I.S.[a]	ΔE_Q[b]	Hi[c]	RI(h)[d]	RI(A)[e]
5	0.442	0.278	0	—	—	—	—	—
20	0.416	0.278	0	0.359	1.104	0	0.23	0.22
40	0.403	0.248	0	0.358	1.074	0	0.18	0.14
60	0.400	0.1 ± 0.2	256 ± 9	—	—	—	—	—
80	0.370	0.05 ± 0.04	485 ± 5	0.37	0.03 ± 0.02	451 ± 5	0.9	1.4[f]
100	0.367	0.06 ± 0.01	529 ± 5	—	—	—	—	—

[a] Isomer shift in mm/sec relative to Fe metal.

[b] Quadrupole splitting in mm/sec.

[c] Hyperfine field in kG.

[d] Relative intensity vs type 1, based on peak heights.

[e] Relative intensity vs type 1, based on peak areas.

[f] For 80% Fe, ratios based on height are significantly different from those based on area. This is a strong indication that a model based on only two kinds of Fe is too simplistic. Unfortunately, the data are not good enough to unambiguously determine all the parameters of a more complex model involving a range of sites.

heating a virgin sample and one on cooling through a magnetic field. Since it is known that parasitic ferromagnetism exists for $LaFeO_3$, (*7*) a manifestation of anisotropic superexchange, cooling through T_N in a magnetic field must align this magnetization with the field.

The hysteresis results from the fact that the coercivity (from crystal anisotropy) of the parasitic magnetization component goes to zero at T_N. Therefore even a small field can irreversibly magnetize all particles on cooling through T_N. Further cooling continues to increase the magnetization as thermal randomization becomes less important. The same effect occurs with 10% Ru in $LaFeO_3$, but at a lower T_N. Finally at 20% Ru, parasitic magnetization has decreased, no hysteresis occurs, and T_N is decreased further. Note that as the temperature is lowered, the magnetization goes through a maximum, rather than increasing steadily. This appears to correspond to some more complex magnetic structure, intermediate between parasitic ferromagnetism and well-behaved antiferromagnetism. As a rough approximation, T_N decreases ~100°K for every 10% Ru. Thus, Ru^{3+} appears to be somewhat less efficient, compared to Al^{3+} in $LaAl_xFe_{1-x}O_3$, (*8*) in decreasing magnetic interactions on the Fe sublattice. From the susceptibility and magnetization plots, an approximate plot of T_N vs x can be constructed and is shown in Fig. 7.

Mössbauer

Mössbauer spectra were all taken at room temperature. Unfortunately, some of the compounds are magnetically ordered at room temperature, and this complicates interpretation. Nevertheless, we felt that unambiguous assignment of the Fe valence state would be possible. The data are shown in Fig. 8 and listed in Table IV. At $LaFeO_3$, the six-line spectra is as expected for a magnetically ordered $AFeO_3$ perovskite (*7*). At 20% Ru, the spectra show two kinds of magnetically ordered Fe^{3+}, probably resulting from nonequivalent Fe^{3+} atoms at this Fe/Ru ratio (*9*). The data have been fit to two kinds, but a distribution over more than two is probable. The small quadrupole splitting is consistent with the nearly cubic symmetry.[2] Note, however, that even if the solid solution were strictly cubic, a nonzero electric field gradient will result from the fact that all Fe atoms cannot have the same ionic environment—some will have more Ru neighbors than others. At 40% Ru, the Néel temperature is close to room temperature, making the data too complicated to resolve. At 60 and 80% Ru, where the samples are clearly paramagnetic at room temperature, a simpler spectra results and again, at least two kinds of Fe^{3+} are indicated. The large quadrupole splitting suggests that a large deviation from cubic symmetry is present, as is supported by the crystallographic data. At a very low concentration of Fe, 5%, the spectra is consistent with only one kind of Fe^{3+}, presumably because nearly all the Fe^{3+} have all Ru nearest neighbors.

For all the solid solutions, the isomer shift is consistent with high-spin, octahedral Fe^{3+} (*10*).

Discussion

We are able to draw a number of conclusions from the data. Electrically, the $LaRu_xFe_{1-x}O_3$ system behaves much like its $LaRu_xGa_{1-x}O_3$ counterpart—a small amount of Fe^{3+} is able to destroy the metallic conductivity of $LaRuO_3$. No discontinuous electrical behavior vs composition and no semiconductor–metal transition vs temperature is found for any composition. Mössbauer isomer shifts and high magnetic moments for the paramagnetic solid solutions identify the Fe as high-spin, octahedral Fe^{3+}. Apparently the combination $Ru^{3+} + Fe^{3+}$ is more stable than $Ru^{4+} + Fe^{2+}$. Magnetically, Ru^{3+} appears to be much more effective at reducing the strength of the magnetic interactions in $LaFeO_3$ than Fe^{3+} is in increasing the weak antiferromagnetic interactions in $LaRuO_3$.

[2] A referee has correctly pointed out that a high unit cell symmetry does not necessarily translate to a high site symmetry. However, as shown in P. Coppens *et al., Acta Cryst.* **19**, 524 (1965), the distortion in $LnFeO_3$ perovskites is borne almost entirely by the Ln^{+3} ion, while the FeO_6 octahedra are quite symmetrical.

Acknowledgments

We would like to acknowledge helpful discussions with H. S. Jarrett and the assistance of C. M. Foris of the X-ray lab.

References

1. R. J. BOUCHARD AND J. F. WEIHER, *J. Solid State Chem.* **4**, 80 (1972).
2. R. J. BOUCHARD, J. F. WEIHER, AND J. L. GILLSON, *J. Solid State Chem.* **6**, 519 (1973).
3. F. GALASSO AND W. DARBY, *Inorg. Chem.* **4**, 71 (1965).
4. M. MAREZIO AND P. D. DERNIER, *Mat. Res. Bull.* **6**, 23 (1971).
5. G. V. SUBBA RAO, B. M. WANKLYN, AND C. N. R. RAO, *J. Phys. Chem. Solids* **32**, 345 (1971).
6. T. C. GIBB, R. GREATREX, N. N. GREENWOOD, AND K. G. SNOWDON, *J. Solid State Chem.* **14**, 193 (1975).
7. D. TREVES, *J. Appl. Phys.* **36**, 1033 (1965).
8. J. TRAFF, *Phys. Status Solidi* **34**, K139 (1969).
9. See G. H. JONKER, *Physica* **22**, 707 (1956) for the distribution probabilities of nearest neighbors.
10. J. DANON, *in* "Chemical Applications of Mössbauer Spectroscopy" (V. I. Goldanskii and R. H. Herber, Eds.), p. 166, Academic Press, New York, 1968.